Stem Cell Reports
Article

ISSCR

OPEN ACCESS

Postnatal Calvarial Skeletal Stem Cells Expressing PRX1 Reside Exclusively in the Calvarial Sutures and Are Required for Bone Regeneration

Katarzyna Wilk,[1,6] Shu-Chi A. Yeh,[1,2,6] Luke J. Mortensen,[1,2,4,6] Sasan Ghaffarigarakani,[1] Courtney M. Lombardo,[1,5] Seyed Hossein Bassir,[1] Zahra A. Aldawood,[1] Charles P. Lin,[2,3,*] and Giuseppe Intini[1,3,*]

[1]Department of Oral Medicine, Infection, and Immunity, Harvard School of Dental Medicine, Boston, MA 02115, USA
[2]Advanced Microscopy Program, Center for Systems Biology and Wellman Center for Photomedicine, Massachusetts General Hospital, Harvard Medical School, Boston, MA 02114, USA
[3]Harvard Stem Cell Institute, Cambridge, MA 02138, USA
[4]Regenerative Bioscience Center, Rhodes Center for ADS, and College of Engineering, University of Georgia, Athens, GA 30602, USA
[5]University of Florida College of Dentistry, Gainesville, FL 32608, USA
[6]Co-first author
*Correspondence: lin@helix.mgh.harvard.edu (C.P.L.), giuseppe_intini@hsdm.harvard.edu (G.I.)
http://dx.doi.org/10.1016/j.stemcr.2017.03.002

SUMMARY

Post-natal skeletal stem cells expressing PRX1 (pnPRX1$^+$) have been identified in the calvaria and in the axial skeleton. Here we characterize the location and functional capacity of the calvarial pnPRX1$^+$ cells. We found that pnPRX1$^+$ reside exclusively in the calvarial suture niche and decrease in number with age. They are distinct from preosteoblasts and osteoblasts of the sutures, respond to WNT signaling in vitro and in vivo by differentiating into osteoblasts, and, upon heterotopic transplantation, are able to regenerate bone. Diphtheria toxin A (DTA)-mediated lineage ablation of pnPRX1$^+$ cells and suturectomy perturb regeneration of calvarial bone defects and confirm that pnPRX1$^+$ cells of the sutures are required for bone regeneration. Orthotopic transplantation of sutures with traceable pnPRX1$^+$ cells into wild-type animals shows that pnPRX1$^+$ cells of the suture contribute to calvarial bone defect regeneration. DTA-mediated lineage ablation of pnPRX1$^+$ does not, however, interfere with calvarial development.

INTRODUCTION

The cranial vault undergoes intramembranous bone formation and provides mechanical support and protection for the brain. Important elements of the calvarial structure are the sutures that narrow during appositional bone growth and remain as an active site of bone formation during calvarial development. In 2007, Lana-Elola et al. showed that during calvarial development, mesenchymal cells of the sutures differentiate to form calvarial bone and their differential fate depends on positioning, with cells occupying the midline of the suture mesenchyme less prone to differentiation. In 2014, Ouyang et al. published a thorough observation about PRX1-expressing cells of the postnatal calvaria, showing that these cells have qualities of skeletal stem cells (SSCs), reside in the calvarial sutures, and are distinct from postnatal cells of the sutures expressing Collagen 1 (COL1). Zhao et al. (2015) and, more recently, Maruyama et al. (2016) showed that various populations of SSCs reside in postnatal calvarial sutures, supporting the logic that the stem cell niche of the calvaria is contained in the suture mesenchyme. Additional research about SSCs of the calvaria and their niche is required to devise therapeutic strategies which, by targeting a specific population of SSCs, can promote calvarial bone regeneration or perturb the development of craniofacial malformations, such as craniosynostosis.

The pair-related homeobox gene *Prx1* (also known as *Prrx1*) is a transcription factor that is highly expressed during limb bud formation and craniofacial development (Martin and Olson, 2000). PRX1-expressing cells and their postnatal progeny also have a central role in bone homeostasis and fracture repair since inactivation of RANKL (receptor activator of nuclear factor κB ligand) expression in these cells causes osteopetrosis (Xiong et al., 2011) and inactivation of BMP2 (bone morphogenetic protein 2) expression generates a low-bone-mass phenotype, with bones prone to factures and unable to repair (Tsuji et al., 2006). In culture, PRX1-expressing cells isolated from the periosteum of postnatal long bones (Kawanami et al., 2009) or postnatal calvaria (Ouyang et al., 2014) can differentiate into chondroblasts and osteoblasts upon induction. Additional studies show that PRX1 averts differentiation of cells into committed osteoblasts (Lu et al., 2011) or adipocytes (Du et al., 2013). Together, the evidence suggests that expression of *Prx1* is a unique marker to identify and characterize SSCs of the calvarial bones. We therefore hypothesize that postnatal cells expressing PRX1 (pnPRX1$^+$) of the calvaria represent an SSC population that resides exclusively in the sutures and is required for calvarial bone regeneration. Using intravital microscopy (IVM) (Lo Celso et al., 2009), we performed lineage-tracing analyses and lineage-ablation analyses to show that pnPRX1$^+$ cells reside exclusively in

the sutures, are required for regeneration of calvarial bone defects, and are dispensable for postnatal calvarial development.

RESULTS

pnPRX1$^+$ Cells of the Calvaria Reside in Calvarial Sutures and Decrease in Number with Age

Prx1-creER-EGFP transgenic mice expressing GFP (EGFP) under the control of the Prx1 promoter (Kawanami et al., 2009) were imaged by IVM (Lo Celso et al., 2009) to investigate the presence of pnPRX1$^+$ cells in calvarial bone and calvarial sutures.

We found pnPRX1$^+$ cells located exclusively in the posterior frontal, coronal, sagittal, and lambdoid sutures (Figure 1A). pnPRX1$^+$ cells were not found in other craniofacial sutures (Figure 1B), the calvarial periosteum, or the dura mater (Figure S1). In addition, pnPRX1$^+$ cells were not present in the calvarial bone marrow of mature mice (Figure 1Cα), where postnatal osteoblasts expressing COL1 (Kern et al., 2001) (pnCOL1$^+$ cells) are commonly found (Figure 1Cβ). Within the coronal suture, pnPRX1$^+$ cells were quantified at 8, 16, 24, and 32 weeks of age and data analysis showed a 75% reduction of cells between 8 and 32-week-old animals (Figure 1D). We also quantified the total cellularity of the suture to determine whether there was a reduction in cell density and found no difference in total cell numbers between 8- and 32-week-old animals (Figure S2). These data confirm that pnPRX1$^+$ cells distinctively populate the calvarial sutures and that their number decreases with age.

pnPRX1$^+$ Cells of the Calvarial Sutures Are Distinct from Preosteoblasts and Osteoblasts of the Calvaria

Given the localization of pnPRX1$^+$ cells, we hypothesized that they are distinct from postnatal preosteoblasts expressing Osterix (pnOSX$^+$ cells) (Nakashima et al., 2002). To test this hypothesis, we imaged Prx1-creER-EGFP mice crossed with Osterix_mCherry reporter mice (Strecker et al., 2013). Our data reveal that pnPRX1$^+$ cells do not co-express OSX in the calvarial sutures (Figure 1Eα). Consistent with Ouyang et al. (2014), pnPRX1$^+$ cells are also distinct from postnatal osteoblasts expressing COL1 (pnCOL1$^+$ cells [Kalajzic et al., 2002; Kern et al., 2001]). In fact, pnCOL1$^+$ cells were detected by the osteogenic fronts of the sutures but were never found within the suture space mesenchyme (Figure 1Eβ). We conclude that pnPRX1$^+$ cells of the calvarial sutures are distinct from preosteoblasts and osteoblasts of the calvaria.

PRX1-Expressing Cells and Their Progeny Are Responsible for the Development of the Calvarial Sutures and Calvarial Bones, and for Regeneration of the Calvarial Bones

We performed lineage-tracing analysis to determine whether PRX1-expressing cells and their progeny are responsible for the development of calvarial sutures. To this end, Prx1-Cre mice (Logan et al., 2002) were crossed with fl/fl tdTOMATO reporter mice (tdTOMATO mice) (Madisen et al., 2010). Coronal sutures were imaged by IVM and tdTOMATO was detected in the suture space, the surrounding periosteum, osteogenic fronts of the suture, and mature bone (as osteocytes) of both neural crest-derived (frontal) (Jiang et al., 2002) and mesoderm-derived (parietal) (Yen et al., 2010) bones of Prx1-cre$^{+/-}$;tdTOMATO$^{+/-}$ mice (Figure 2A). To confirm the results, we crossed the Prx1-Cre mice with transgenic mice able to express diphtheria toxin A (DTA) upon CRE recombination of a loxP-flanked STOP cassette (Voehringer et al., 2008). The Prx1-cre$^{+/-}$;DTA$^{+/-}$ mice at birth (postnatal day 0 [P0]) displayed incomplete development of the frontal bone and lack of development of the parietal, interparietal, and occipital bones (Figure 2Bα). The posterior frontal, coronal, sagittal, and lambdoid sutures were also absent. Gross anatomical inspection revealed impaired limb development in these mice (Figure 2Bβ) and validated our experimental approach, since PRX1 is also expressed in developing limbs (Logan et al., 2002).

These lineage-tracing and lineage-ablation analyses indicate that embryonic cells expressing PRX1, their postnatal progeny, and, possibly, postnatal cells expressing PRX1 cells are responsible for development of neural crest-derived (i.e., frontal bone) (Jiang et al., 2002) and mesoderm-derived (i.e., parietal bone) (Yen et al., 2010) calvarial bones. Thus, expression of PRX1 identifies a population of cells of mixed neural crest and mesoderm origins.

To test whether PRX1-expressing cells and their progeny also regenerate calvarial bones, we evaluated their contribution to regeneration of a subcritical defect (Cowan et al., 2004) in the frontal and parietal bones of 8-week-old Prx1-cre$^{+/-}$;tdTOMATO$^{+/-}$ animals (Figure 2C). IVM analysis of the regenerated bones shows cells expressing tdTOMATO in the defects 5 days post surgery, increased progeny 10 days post surgery, and in bone formed 30 days post surgery. We concluded that progeny of embryonic cells expressing PRX1 and possibly pnPRX1$^+$ cells contribute to the regeneration of neural crest-derived (frontal) (Jiang et al., 2002) and mesoderm-derived (parietal) (Yen et al., 2010) calvarial bones. Thus, postnatal expression of PRX1 may identify a population of cells that contribute to or are directly responsible for calvarial bone regeneration.

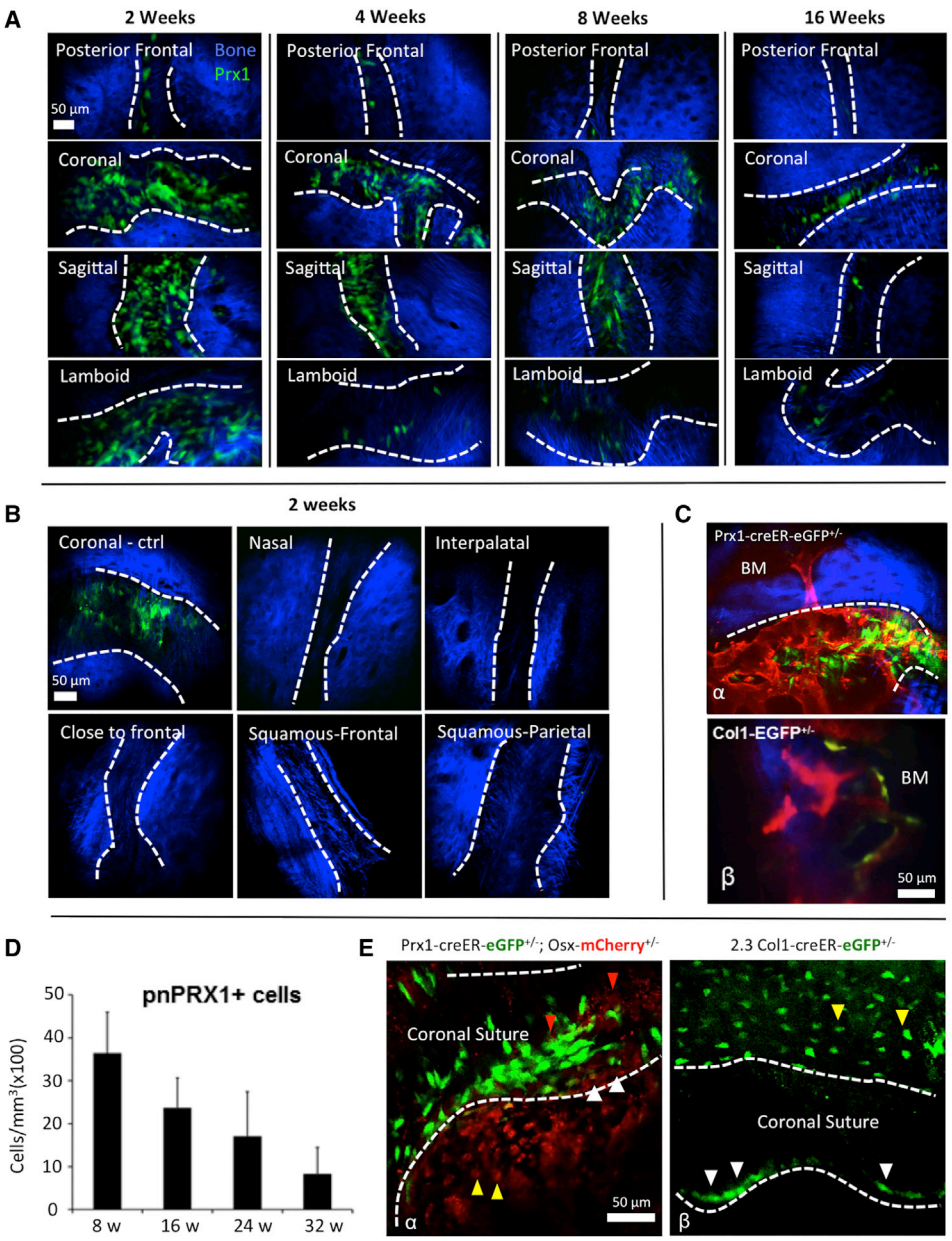

Figure 1. pnPRX1^{+} Cells of the Calvaria Are Found in the Calvarial Sutures, Decline in Number with Age, and Are Distinct from Preosteoblasts and Osteoblasts

(A) Visualization of EGFP-expressing cells in calvarial sutures of PRX1-creER-EGFP$^{+/-}$ mice, at different ages.

(B) Visualization of EGFP-expressing cells in other craniofacial sutures of PRX1-creER-EGFP$^{+/-}$ mice in 2-week-old animals. Coronal sutures were used as control (ctrl).

(C) (α) Intravital examination of the calvarial bone marrow space (BM) in 8-week-old Prx1-creER-EGFP$^{+/-}$ mice. Dashed lines demarcate the suture space. (β) Intravital examination of the calvarial bone marrow space in 8-week-old Col1-EGFP$^{+/-}$ mice.

(D) Quantification of EGFP-expressing cells (pnPRX1^{+} cells) in coronal sutures of Prx1-creER-EGFP$^{+/-}$ mice at different ages (n = 3–5 mice/group). The average number of cells/mm^3 ± SD are reported.

(E) Visualization of EGFP-expressing cells and mCherry-expressing cells in the coronal suture of 2-week-old Prx1-creER-EGFP$^{+/-}$;Osx-mCherry$^{+/-}$ mice. OSX is expressed in osteocytes (yellow arrowheads), cells at the osteogenic front (white arrowheads), and a few cells in the suture (red arrowheads). Unlike Prx1-expressing cells in the suture, Col1-EGFP-expressing cells are only expressed in osteocytes (yellow arrowheads) and cells at the osteogenic front (white arrowheads). Dashed lines demarcate the suture space.

Scale bars, 50 µm.

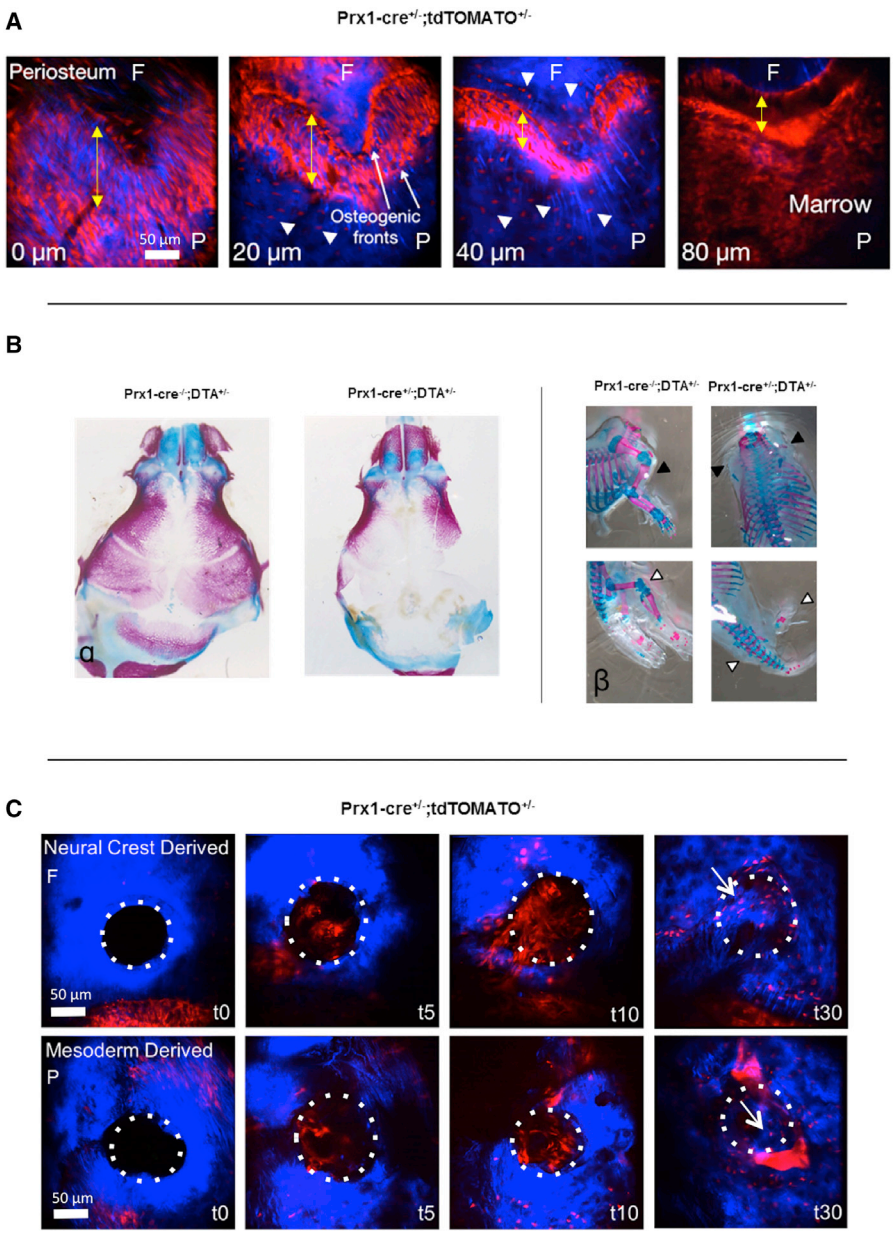

Figure 2. PRX1-Expressing Cells and Their Progeny Are Responsible for the Development of the Calvarial Sutures and Calvarial Bones, and for the Regeneration of the Calvarial Bones

(A) Lineage-tracing analysis of PRX1-expressing cells of the coronal suture in 6- to 8-week-old PRX1-cre$^{+/-}$;tdTOMATO$^{+/-}$ mice (transversal sections at 0, 20, 40, and 80 µm from the periosteal surface). Bone is visualized by second harmonic generation (blue). Frontal bone (F), parietal bone (P), suture space (yellow double arrow), osteogenic fronts (white arrows), and osteocytes (white arrowhead) are indicated (n = 3 mice).

(B) Effects of global ablation of Prx1^{+} cells during embryogenesis in newborn (P0) Prx1-cre;DTA mice. (α) Calvarial bones. (β) Forelimb (black arrowheads) and hindlimb (white arrowheads) (n = 4–6 mice/group).

(C) Lineage-tracing analysis of the PRX1-expressing cells of the neural crest-derived frontal (F) and mesoderm-derived parietal (P) bones during bone regeneration in 8-week-old PRX1-cre$^{+/-}$;tdTOMATO$^{+/-}$ mice. Images were acquired at the time of the defect creation (t0), 5 days later (t5), 10 days later (t10), and 30 days later (t30) to show Prx1 progeny migrating into the defect (white dotted lines) and forming new bones as osteocytes (white arrows) (n = 3 mice).

Scale bars, 50 µm.

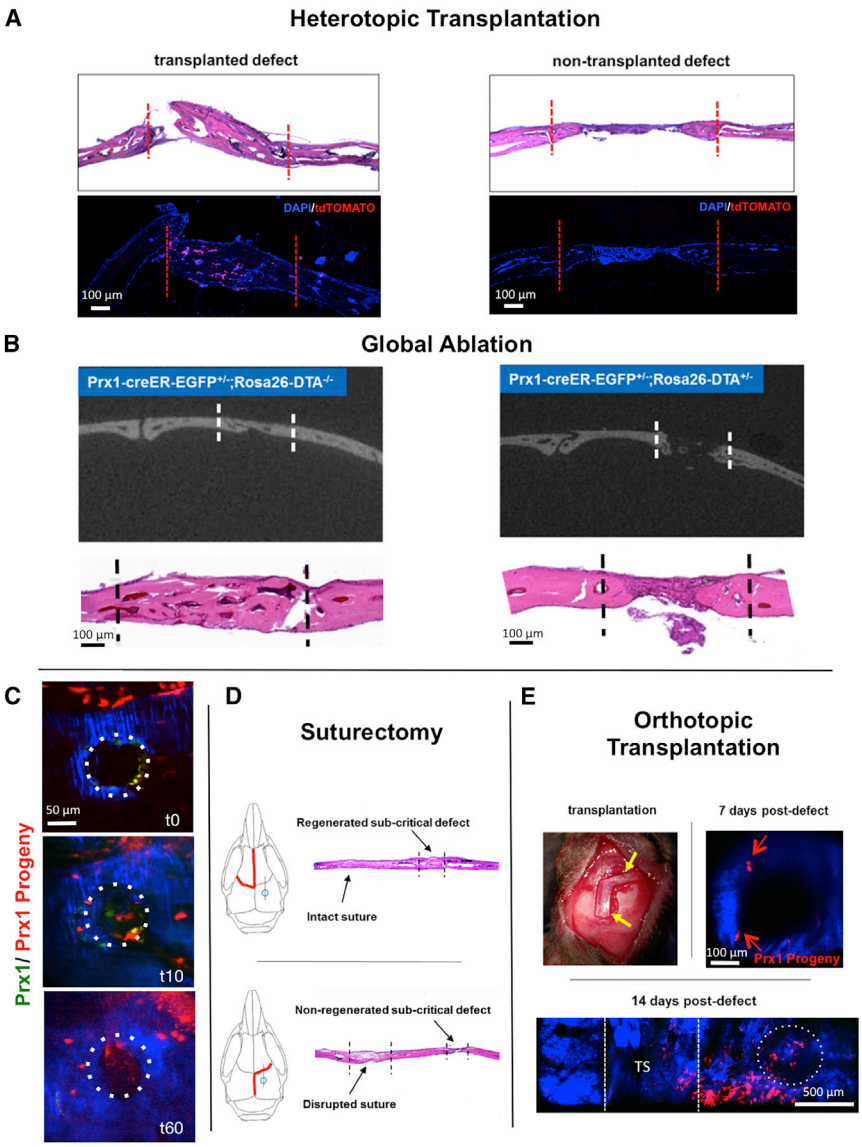

Figure 3. pnPRX1$^+$ Cells of the Calvaria Can Regenerate Bone and Are Required for Calvarial Bone Regeneration, and Calvarial Sutures Are Their Exclusive Niche

(A) Lineage-tracing analysis of pnPRX1$^+$ cells upon heterotopic transplantation of minced sutures from Prx1-creER-EGFP$^{+/-}$;tdTOMATO$^{+/-}$ mice into critical-size calvarial bone defects created in wild-type mice (C57BL/6). Bone defects are identified by the red dashed lines (n = 2–3 mice/group). Scale bars, 100 µm.

(B) Micro-computed tomography and histological sections of calvarial bones dissected 28 days after subcritical calvarial defect surgery (0.5 mm in diameter) in the presence (left) (mice treated with tamoxifen but not carrying the DTA transgene) and absence (right) (mice treated with tamoxifen and carrying the DTA transgene) of pnPRX1$^+$ cells. Dashed lines demarcate the calvarial subcritical bone defect (n = 6 mice). Histology scale bars, 100 µm.

(C) Interval Lineage-tracing analysis of pnPRX1$^+$ cells in defect healing (100 µm in diameter, white dotted lines) using 8-week-old PRX1-creER$^{+/-}$;tdTOMATO$^{+/-}$ mice. Images acquired at the time of defect creation (t0), five days later (t5), 10 days later (t10) (n = 6 mice), and 60 days later (t60) (n = 2 mice). Scale bars, 50 µm.

(D) (Upper) Suturectomy of the frontal and left coronal sutures (thick red lines) with a subcritical bone defect created in the right parietal bone. (Lower) Suturectomy of the sagittal and right coronal sutures (thick red lines) with a subcritical bone defect created in the right parietal bone. Thin red lines across the defects indicate the sagittal planes of the histological sections shown. Black dashed lines in the histological sections indicate suturectomy sites and regeneration sites (n = 5 mice/group).

(E) Lineage-tracing analysis of pnPRX1$^+$ cells upon orthotopic transplantation of coronal and sagittal sutures from Prx1-creER-EGFP$^{+/-}$;tdTOMATO$^{+/-}$ mice into suturectomy sites of wild-type mice (C57BL/6). (Upper left) Orthotopic transplantation of the coronal and sagittal sutures (yellow arrows). (Upper right) Day 7 post parietal, subcritical bone defect surgery (horizontal views at 60 µm from the periosteal surface). Red arrows point to tdTOMATO-expressing cells detected in the defect. Scale bars, 100 µm. (Lower) Day 14 post defect surgery. Horizontal rendering of the transplanted suture (TS, white dashed lines) and the bone defect (white dotted circle). Blue and red signals are shown in maximum-intensity projection over 20 µm of depth (n = 2 mice). Scale bars, 100 µm (upper) and 500 µm (lower).

pnPRX1$^+$-Expressing Cells of the Calvaria Are Required for Calvarial Bone Regeneration

To determine whether pnPRX1$^+$ cells of the sutures can mediate bone regeneration, we transplanted coronal sutures obtained from Prx1-creER-EGFP$^{+/-}$;tdTOMATO$^{+/-}$ mice into a critical-size calvarial bone defect (2 mm in diameter) (Cowan et al., 2004) of wild-type mice (C57BL/6) (heterotopic transplantation, Figure 3A). Wild-type hosts were then injected with tamoxifen to induce tdTOMATO expression in the progeny of the transplanted pnPRX1$^+$ cells within the newly regenerated bone. Results show that transplanted suture tissue (heterotopic site) is able to regenerate bone rather than suture-like structures and that pnPRX1$^+$ cells of the sutures give rise to the majority of the cells incorporated into the newly formed bone.

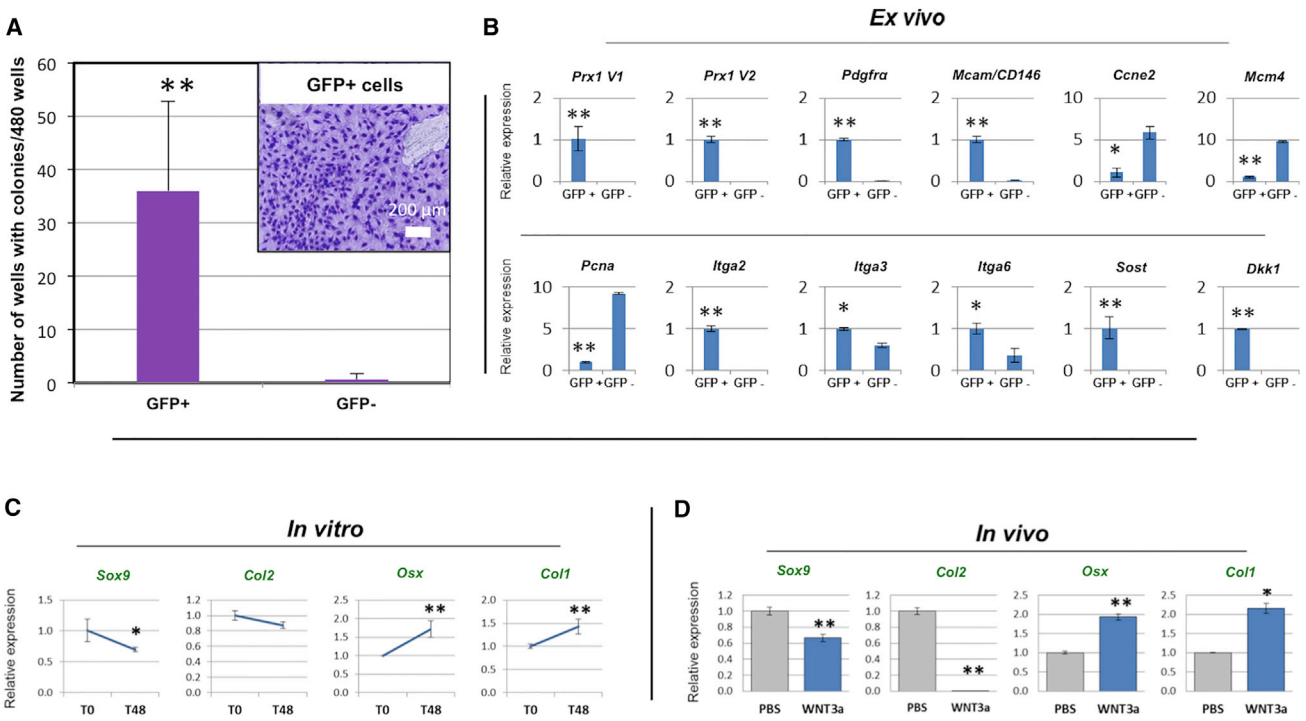

Figure 4. pnPRX1$^+$ Cells of the Calvaria Present with Qualities of Skeletal Stem Cells

(A) In vitro, pnPRX1$^+$ cells (EGFP$^+$) and EGFP$^-$ cells isolated from the calvarial sutures of 4-week-old Prx1-creER-EGFP$^{+/-}$ mice were cultured at 1 cell/well in a 96-well plate. Colony-forming units (CFU) were counted after 3 weeks and the average CFU/experiment ± SD are reported (n = 3 independent experiments). **p < 0.01. The inset shows the colony formed by the pnPRX1$^+$ cells. Scale bar, 200 µm.

(B) Ex vivo qRT-PCR analysis of pnPRX1$^+$ cells (GFP$^+$) and EGFP$^-$ cells isolated from the calvarial sutures of 4-week-old Prx1-creER-EGFP$^{+/-}$ mice (n = 3 independent experiments). *p < 0.05, **p < 0.01. EGFP$^+$ and EGFP$^-$ validation screen shows higher levels of expression of both transcriptional variants of Prx1 detected in EGFP$^+$ cells. Relative expression values ± SD are reported.

(C) Osteodifferentiation of pnPRX1$^+$ cells 48 hr after treatment with rmWNT3a in vitro (n = 3 independent experiments). Relative expression values ± SD are reported. *p < 0.05, **p < 0.01.

(D) Osteodifferentiation of pnPRX1$^+$ cells 24 hr after treatment with rmWNT3a in vivo (n = 5–6 mice/group). Relative expression values ± SD are reported. *p < 0.05, **p < 0.01.

To expand on the data, we used Prx1-CreEr-EGFP$^{+/-}$; DTA$^{+/-}$ mice to conditionally ablate pnPRX1$^+$ cells during bone regeneration. Preliminary tests showed that 5 days of tamoxifen treatment in these mice results in >80% pnPRX1$^+$ cell ablation efficiency (Figure S3). We observed that in a subcritical calvarial bone defect model (0.5 mm in diameter), 8- to 10-week-old Prx1-creER-EGFP$^{+/-}$;DTA$^{+/-}$ mice treated with tamoxifen showed that ablation of pnPRX1$^+$ cells impairs regeneration of the defects (Figure 3B). Using IVM, we further demonstrated that pnPRX1$^+$ cells directly contribute to bone regeneration of the subcritical calvarial defect in 8-week-old Prx1-creER-EGFP$^{+/-}$;tdTOMATO$^{+/-}$ mice (Figure 3C), where pnPRX1$^+$ cells (EGFP$^+$) and their progeny (tdTOMATO$^+$) migrated into the defects by day 10 after the defect was made. We concluded that pnPRX1$^+$ cells are required to regenerate calvarial bone. However, since DTA globally ablates pnPRX1$^+$ cells, further studies are necessary to isolate the contributions of pnPRX1$^+$ cells specifically localized to the calvarial sutures in regeneration of calvarial defects.

The Calvarial Suture Is the Exclusive Niche of the pnPRX1$^+$ Cells

To confirm that only the pnPRX1$^+$ cells of the calvarial sutures contribute to the regeneration of calvarial defects and therefore that the calvarial suture is their exclusive niche, we isolated the contribution of other potential sources of pnPRX1$^+$ cells. First, we created a subcritical calvarial defect in the parietal bone of the calvaria while concomitantly performing suturectomy (without affecting the underlying dura). Previously we showed that parietal bone defects are unable to heal if a suturectomy of the surrounding coronal and sagittal sutures is performed concomitantly to the creation of the defect. The results demonstrate that subcritical-size bone defects are unable to heal in absence of surrounding intact sutures (Figure 3D). In a second

Table 1. qRT-PCR TaqMan Gene Expression Primer Assay Codes

Gene	TaqMan Assay Code
TBP	Mm00446971_m1
Tubb5	Mm00495806_g1
B-actin	Mm02619580_g1
Prx1 V1	Mm00599934_m1
Prx1 V2	Mm01014477_m1
Col2a1	Mm01309565_m1
Sox9	Mm00448840_m1
Mcam/Cd146	Mm00522397_m1
Dkk1	Mm00438422_m1
Axin2	Mm00443610_m1
Col1A1	Mm00801666_g1
Osx/Sp7	Mm04209856_m1
$Sost^{-}$ Sclerostin	Mm04208528_m1
Gli1	Mm00494654_m1
Pdgfr alpha	Mm00440701_m1
CCNE2	Mm00438077_m1
MCM4	Mm00725863_s1
PCNA	Mm00448100_g1
Itga2	Mm00434371_m1
Itga3	Mm00442910_m1
Itga6	Mm00434375_m1

experiment, we transplanted the sagittal and right coronal suture from Prx1-creER-EGFP$^{+/-}$;tdTOMATO$^{+/-}$ mice into wild-type mice (orthotopic transplantation, Figure 3E). Six weeks after transplantation, host mice (wild-type) were treated with tamoxifen and a subcritical-size defect was created in the parietal bone surrounded by the transplanted sutures. IVM analysis showed that progeny of the transplanted pnPRX1^{+} cells (tdTOMATO^{+}) appear within the deepest portion of the parietal defect 7 days after surgery. Fourteen days after surgery, we saw progeny of the transplanted pnPRX1^{+} cells incorporated in the newly regenerated bone and in the nearby tissue. tdTOMATO-expressing cells were not seen in the contralateral parietal bone. Therefore, since a regional suturectomy averts bone regeneration and pnPRX1^{+} cells of orthotopically transplanted sutures contribute to bone regeneration, we can conclude that pnPRX1^{+} cells of the sutures are the PRX1-expressing cells required for intramembranous bone regeneration and that the calvarial suture is their exclusive niche.

pnPRX1^{+} Cells of the Calvarial Sutures Present with Qualities of Skeletal Stem Cells

To characterize pnPRX1^{+} cells as SSC's, we first performed in vitro clonogenic assays and confirmed that pnPRX1^{+} cells isolated from the calvarial sutures of 4-week-old Prx1-creER-EGFP$^{+/-}$ mice are clonogenic (Figure 4A). Ex vivo gene expression analysis of pnPRX1^{+} cells (EGFP^{+}) and EGFP^{-} cells isolated from calvarial sutures of 4-week-old Prx1-creER-EGFP$^{+/-}$ mice (Figure 4B; Table 1) supports that EGFP^{+} cells present with a well-defined SSC profile. We observed an upregulation of *Pdgfrα* and *Mcam/Cd146*, two genes associated with SSCs (Chan et al., 2015; Houlihan et al., 2012; Pinho et al., 2013; Sacchetti et al., 2007). pnPRX1^{+} cells also express low levels of genes associated with cell cycle progression, chromosome segregation, and DNA replication such as *Ccne2*, *Mcm4*, and *Pcna* which are characteristic of quiescent cells (Cheung and Rando, 2013). Higher levels of *Itga2*, *Itga3*, and *Itga6* genes associated with stem cell homing and anchoring to the extracellular matrix of the niches (Chen et al., 2013; Cheung and Rando, 2013) were also detected in pnPRX1^{+} cells. Finally, pnPRX1^{+} cells express high levels of *Dkk1* and *Sost*, two inhibitors of the WNT signaling pathway (Baron and Kneissel, 2013) that are suggested to contribute to the maintenance of the undifferentiated quiescent status of the pnPRX1^{+} cells.

Canonical WNT signaling is significantly active during craniofacial bone formation (Mani et al., 2010). Therefore, to test the differentiation potential of pnPRX1^{+} cells, we stimulated pnPRX1^{+} cells cultured in vitro with recombinant mouse WNT3a (rmWNT3a) for 48 hr and found an increase in the expression of osteoblast-specific markers and reduction in the expression of *Sox9*, a well-defined chondroblastic marker (Figure 4C; Table 1). To confirm this finding, we injected rmWNT3a locally to calvarial sutures of Prx1-creER-EGFP$^{+/-}$ mice and found that pnPRX1^{+} cells isolated 24 hr after treatment presented the same gene expression variations observed in pnPRX1^{+} cells treated in vitro (Figure 4D; Table 1). Validation of the subperiosteal local injection was confirmed by IVM (Figure S4).

The qualities of pnPRX1^{+} cells, typically seen in SSCs, support our hypothesis that pnPRX1^{+} cells represent a quiescent population of cells of the sutures that upon appropriate stimulation (i.e., a WNT canonical agonist) can exit the undifferentiated status and differentiate into osteoblasts.

In the Postnatal Suture, PRX1-Expressing Cells Overlap with GLI1-Expressing Cells

In adult mice, GLI1 marks the vast majority of the suture mesenchyme with the exception of few cells at the osteogenic fronts (Zhao et al., 2015). Our model shows

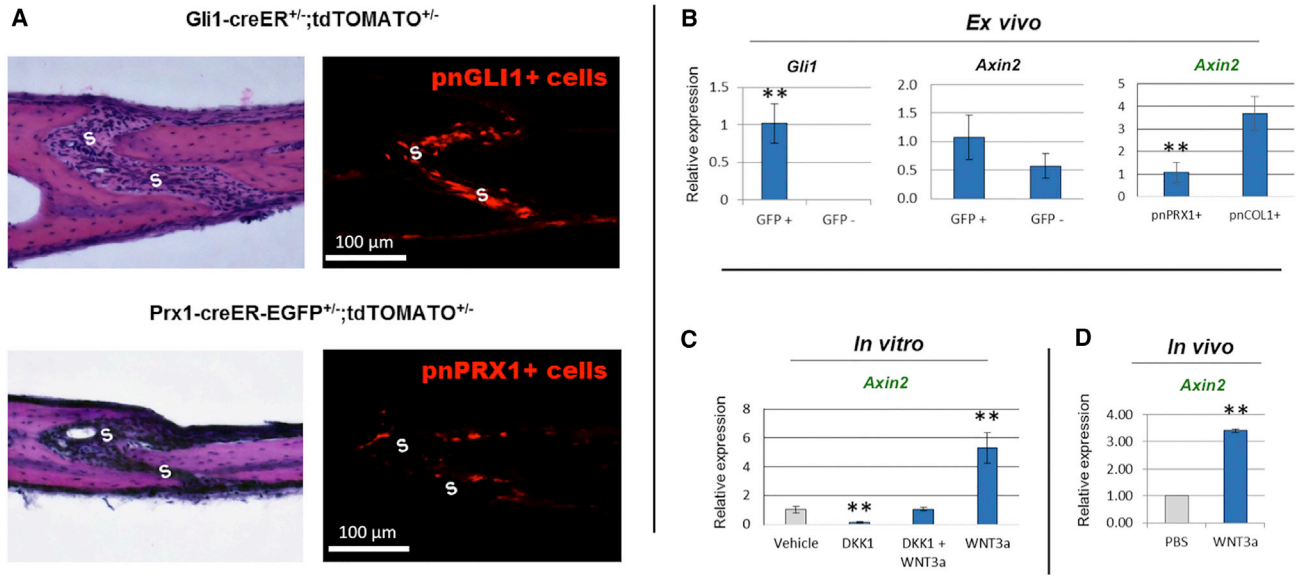

Figure 5. In the Postnatal Suture, PRX1-Expressing Cells Overlap with GLI1-Expressing Cells

(A) Comparative evaluation of tdTOMATO expression in 4-week-old Prx1-creER-EGFP$^{+/-}$;tdTOMATO$^{+/-}$ and Gli1-creER$^{+/-}$;tdTOMATO$^{+/-}$ mice treated with tamoxifen for 5 days (short-pulsing). S, suture space (n = 2 mice). Scale bars, 100 µm.

(B) Ex vivo qRT-PCR analysis of *Gli1* and *Axin2* expression in pnPRX1^{+} cells (EGFP^{+}), (EGFP^{-}), and in pnCOL1^{+} cells isolated from the sutures (n = 3 independent experiments). Relative expression values ± SD are reported. **p < 0.01.

(C) In vitro qRT-PCR analysis of *Axin2* expression in cells treated with rmWNT3a and rmDKK1 (n = 3 independent experiments). Relative expression values ± SD are reported. **p < 0.01.

(D) In vivo qRT-PCR analysis of *Axin2* expression in pnPRX1^{+} cells treated with rmWNT3a (n = 5–6 mice/group). Relative expression values ± SD are reported. **p < 0.01.

that pnPRX1^{+} cells occupy a more discrete position within the suture space (Figure 1). To confirm this differential localization, we compared the expression of tdTOMATO in short-pulsed 4-week-old Prx1-creER-EGFP$^{+/-}$;tdTOMATO$^{+/-}$ mice and in short-pulsed 4-week-old Gli1-creER$^{+/-}$;tdTOMATO$^{+/-}$ mice. Results indicate that GLI1 expression marks a wider population of cells within the sutural space (Figure 5A). Quantification of the percentage of cells of the Prx1-creER-EGFP$^{+/-}$;tdTOMATO$^{+/-}$ suture expressing tdTOMATO after short-pulsing of tamoxifen confirms that this difference is not due to a lower recombination efficiency of the Prx1-creER-EGFP transgene (Figure S5). Furthermore, in situ hybridization confirms that expression of endogenous *Prx1* is recapitulated by the expression of the Prx1-creER-EGFP transgene (Figure S6). We then hypothesized that pnPRX1^{+} cells also express *Gli1*. Ex vivo qRT-PCR of the EGFP^{+} cells and EGFP^{-} cells isolated from the coronal and sagittal sutures of Prx1-creER-EGFP$^{+/-}$ mice shows that pnPRX1^{+} cells (EGFP^{+}) express higher levels of *Gli1* compared with EGFP^{-} cells of the suture (Figure 5B; Table 1). These data indicate that there is an overlap between pnGLI1^{+} and pnPRX1^{+} cell populations, with PRX1 expressed in a smaller number of cells within the suture.

Maruyama et al. (2016) showed that there is also an overlap between the AXIN2-expressing cells of the sutures (pnAXIN2^{+}) and the pnGLI1^{+} cells therefore we investigated whether pnPRX1^{+} cells and pnAXIN2^{+} cells are the same stem cell population of the suture. Ex vivo quantitative gene expression analysis reveals no difference in *Axin2* expression levels in pnPRX1^{+} cells compared with the expression levels measured in the entire EGFP^{-} population of the suture (Figure 5B; Table 1). This indicates that expression of *Axin2* in pnPRX1^{+} cells is low. In support of this evidence, we found that expression of *Axin2* is lower in pnPRX1^{+} cells compared with mature osteoblasts of the suture expressing COL1 (pnCOL1^{+} cells of the sutures) (Figure 5B). Since upregulation of *Axin2* is reported to be induced by agonists of WNT signaling (Baron and Kneissel, 2013), we tested whether the expression levels of *Axin2* in pnPRX1^{+} cells could be increased by rmWNT3a. Data show that pnPRX1^{+} cells treated with rmWNT3a in vitro increases *Axin2* expression by ~5-fold (Figure 5C; Table 1). This WNT-specific responsiveness was confirmed by the observed inhibition of *Axin2* expression upon co-treatment with recombinant DKK1 (Figure 5C). In vivo, we found that subperiosteal delivery

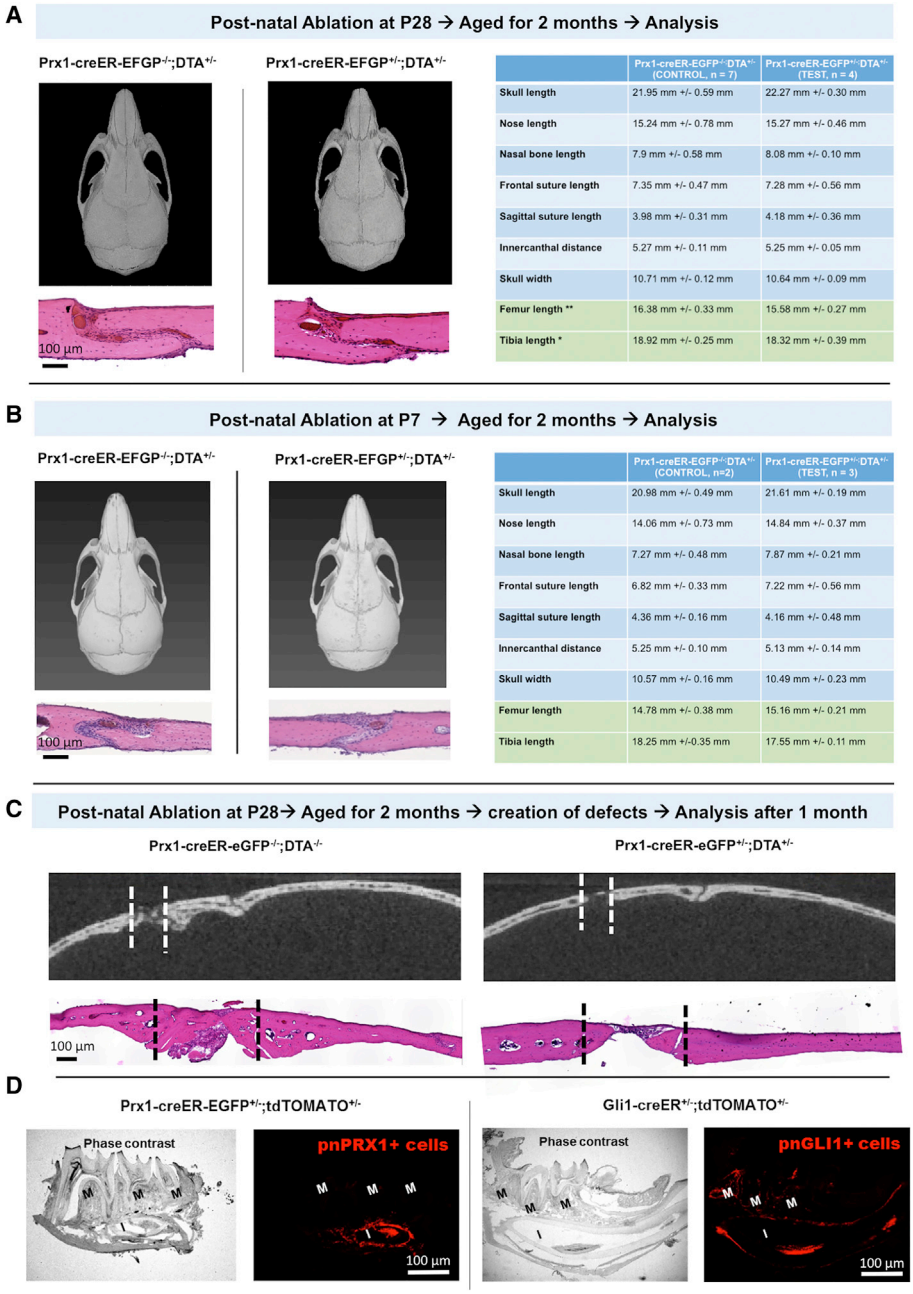

Figure 6. pnPRX1$^+$ Cell Ablation in Young Mice Does Not Interfere with Calvarial Development

(A) Global ablation of pnPRX1$^+$ cells in P28 Prx1-creER-EGFP;DTA mice. (Left) µCT rendering (top) and histological sagittal sections of the coronal sutures (bottom). (Right) Measurements of calvaria, femur, and tibia (n = 4–7 mice/group). Average measurements in mm ± SD are reported. *p < 0.05, **p < 0.01.

(B) Global ablation of pnPRX1$^+$ cells in P7 Prx1-creER-EGFP; DTA mice. (Left) µCT rendering (top) and histological sagittal sections of the coronal sutures (bottom). (Right) measurements of calvaria, femur, and tibia (n = 2–3 mice/group). Average measurements in mm ± SD are reported.

(C) Healing of subcritical defects 2 months after global ablation of pnPRX1$^+$ cells in P28 animals. µCT and histology 28 days after creation of the defect (n = 2 mice/group). Scale bar, 100 µm.

(D) pnPRX1$^+$ cells (left) and pnGLI1$^+$ cells (right) in mandibular bones of Prx1-creER-EGFP$^{+/-}$;tdTOMATO$^{+/-}$ mice and Gli1-creER$^{+/-}$; tdTOMATO$^{+/-}$ mice, respectively (short-pulsing with tamoxifen for 5 days). Phase-contrast images are shown to facilitate anatomical localization. M, molar teeth; I, incisor tooth (n = 2 mice). Histology scale bars, 100 µm.

of rmWNT3a by the calvarial sutures induces osteodifferentiation of pnPRX1$^+$ cells (Figure 4D) and overexpression of *Axin2* in pnPRX1$^+$ cells (Figure 5D; Table 1). We conclude that pnPRX1$^+$ cells represent a cell population with basal levels of expression of AXIN2 and are able to overexpress AXIN2 upon WNT agonist stimulation.

pnPRX1$^+$ Cells of the Suture Are Dispensable for Postnatal Calvarial Development

Previous studies reported that global ablation of pnGLI1$^+$ cells in 4-week-old mice averts craniofacial growth and induces craniosynostosis (Zhao et al., 2015). Since the pnPRX1$^+$ and the pnGLI1$^+$ cell populations of the suture overlap in adult mice and pnPRX1$^+$ cells represent a smaller cell population than pnGLI1$^+$ cells, we hypothesized that ablation of pnPRX1$^+$ cells in 4-week-old mice would generate a less significant phenotype than the one obtained by Zhao et al. We ablated pnPRX1$^+$ cells in P28 Prx1-creER-EGFP$^{+/-}$;DTA$^{+/-}$ mice and analyzed the phenotype of their calvaria and long bones 8 weeks after ablation. Our results show no significant craniofacial phenotype in ablated pnPRX1$^+$ cells of these mice (Figure 6A). Only changes in the length of the femur and the tibia presented a statistically significant difference (Figure 6A). When we ablated pnPRX1$^+$ cells in P7 Prx1-creER-EGFP$^{+/-}$;DTA$^{+/-}$ mice, we observed a similar trend (Figure 6B). Global ablation of pnPRX1$^+$ cells at P28 has a significant effect on the length of the long bones, suggesting that either a significant pool of pnPRX1$^+$ is still needed for development of postnatal long bones or that pnPRX1$^+$ cells have a different role in endochondral bone formation and elongation. Nevertheless, in the calvaria, results differ from the effects observed upon ablation of the widely present pnGLI1$^+$ cells, which results in skull growth arrest and craniosynostosis (Zhao et al., 2015). We show that pnPRX1$^+$ are necessary for subcritical calvarial bone defect regeneration (Figure 6C) and are dispensable for calvarial development.

Since ablation of pnPRX1$^+$ cells has no developmental effects on craniofacial development, we also hypothesized that the distribution of the pnPRX1$^+$ cells across craniofacial tissues is limited. Results of our investigation in tamoxifen short-pulsed 4-week-old Prx1-creER-EGFP$^{+/-}$;tdTOMATO$^{+/-}$ mice support our hypothesis and show that pnPRX1$^+$ cells expressing tdTOMATO are specifically associated only with continuously regenerating tissues, such as the incisor (Zegarelli, 1944; Figure 6D, left). Using the same short-pulsing strategy in 4-week-old Gli1-creER$^{+/-}$;tdTOMATO$^{+/-}$ mice, we identified pnGLI1$^+$ cells in the incisor and in other more metabolically stable tissues, such the molars and the mandibular bone (Figure 6D, right), indicating that *Prx1* expression is more restricted than *Gli1* expression in craniofacial tissues.

DISCUSSION

In this work, we confirm that pnPRX1$^+$ cells of the calvaria presented gene expression profiles of SSC's, are localized to the calvarial suture niche, and are required for calvarial bone regeneration. Global ablation strategies of SSCs do not allow to unequivocally conclude that individual locations (i.e., the sutures) represent their unique niches because absence of the cells from other locations may be responsible for the observed effects. We evaluated the contribution of pnPRX1$^+$ cells of the sutures to calvarial bone regeneration in three different settings (global ablation, regional suturectomy, and orthotopic suture transplantation). This triple experimental strategy allowed us to confirm that sutures are the exclusive niches of the calvarial SSCs expressing PRX1.

Our work demonstrates that expression of PRX1 identifies a subpopulation of the pnGLI1$^+$ cells identified by Zhao et al. (2015). Interestingly, global ablation of pnPRX1$^+$ cells does not result in a major developmental phenotype whereas global ablation of pnGLI1$^+$ cells averts craniofacial growth and induces craniosynostosis. This is expected for two reasons: First, pnPRX1$^+$ cells are discretely distributed across the suture space and their ablation should therefore generate a phenotype less significant than the one obtained by ablation of the widely distributed pnGLI1$^+$ cells. Second, preosteoblasts and osteoblasts of the calvaria have life spans longer than 60 days (Park et al., 2012) and represent a reservoir of cells able to form bone even in absence of their progenitors (in our case pnPRX1$^+$ cells). Thus, the effects of the ablation of SSCs should be seen in long-term studies and may influence craniofacial development only if ablation is performed early enough during development, when a significant pool of SSCs is required. Indeed, when global ablation of PRX1-expressing cells is performed during embryogenesis, we observe an incomplete calvarial bone formation.

Maruyama et al. (2016) did not perform global ablation studies of pnAXIN2$^+$ cells. However, the fact that postnatal OSTERIX-expressing cells co-express AXIN2 (Tan et al., 2014) and the fact that *Osx* is expressed in preosteoblasts (Nakashima et al., 2002; Strecker et al., 2013) suggests that ablation of pnAXIN2$^+$ cells could generate a more significant development phenotype than the one observed in the pnPRX1$^+$ cell ablation studies. Although gene knockout studies cannot be correlated to ablation studies of cells expressing the same genes, the fact that knockout

of *Axin2* generates premature suture closing and craniosynostosis (Yu et al., 2005) suggests that this may in fact be the case.

Our studies indicate that pnPRX1$^+$ cells express low levels of Axin2 and that these levels increase upon WNT agonist stimulation. This result may indicate that either pnPRX1$^+$ cells are the same cells identified by Maruyama et al. (pnAXIN2$^+$ cells) or that pnPRX1$^+$ cells are a subpopulation of pnAXIN2$^+$ cells. Since, at least in long bones, the majority of the postnatal bone cells expressing OSX co-express AXIN2 (Tan et al., 2014), pnPRX1$^+$ cells differ from the OSX-expressing cells of the suture (Figure 1E), and ablation of pnPRX1$^+$ does not interfere with postnatal calvarial development, we speculate that pnPRX1$^+$ cells are a subpopulation of the pnAXIN2$^+$ cells identified by Maruyama et al. Additional studies are required to test this postulation.

In conclusion, our studies showed that pnPRX1$^+$ cells are responsible for calvarial bone regeneration and represent an initial step toward future investigations aiming to identify novel, effective therapies for calvarial malformations and defects.

EXPERIMENTAL PROCEDURES

Animals

Experiments were conducted in compliance with the Guide for the Care and Use of Laboratory Animals (IACUC approval IS00000535). The transgenic mouse lines studied include Prx1-cre mice, Prx1-creER-EGFP mice, Col1-EGFP mice, Osx-mCherry mice, Rosa26LoxP$^{\text{-STOP-loxP-tdtomato}}$ (in this study named tdTOMATO mice), and Rosa26LoxP$^{\text{-STOP-loxP-DTA}}$ (in this study named DTA mice). Only male mice were utilized throughout the reported in vivo studies.

Intravital Microscopy

IVM was performed as previously described (Lo Celso et al., 2009). The excitation beam is focused into the sample plane using a 60× objective lens (numerical aperture = 1). Fluorescence emission is then collected by either confocal or two-photon detectors with proper dichroic and filter settings corresponding to fluorophores of interest. EGFP signals are detected with a 525/38-nm bandpass filter using either two-photon or confocal acquisition excited by a 491-nm laser (Cobolt Calypso). Prx1 progeny expressing tdTOMATO are excited by a Ti:Sapphire laser at 750 nm and detected with a 625/50-nm bandpass filter. Confocal acquisition of Osx-mCherry cells are excited by a 561-nm laser (Cobolt Jive) and detected using a 695/55-nm bandpass filter. For visualization of bones, second harmonic generation (SHG) of collagen is excited by the Ti:Sapphire laser pulsing between 840 and 900 nm according to experimental requirement, and collected by a 435/40-nm bandpass filter.

For visualization of cell distribution in depth, stack images at 1- to 5-μm intervals were acquired via two-photon acquisition. Two-dimensional sections were processed by the *reslice* function of ImageJ.

Quantification of PRX1-Expressing Cells of the Coronal Sutures

Quantification of the PRX1-expressing cells was performed as previously described (Lo Celso et al., 2009) (n = 3–5 mice per time point).

Constitutive Lineage-Tracing Studies

Prx1-cre$^{+/-}$ male mice were crossed with tdTOMATO$^{+/+}$ female mice. The Prx1Cre$^{+/-}$;tdTOMATO$^{+/-}$ male mice were analyzed by IVM at 8 weeks of age (n = 3 mice).

Constitutive Lineage-Ablation Studies

Prx1-cre$^{+/-}$ male mice were crossed with DTA$^{+/+}$ female mice. P0 mice were collected immediately after birth, skinned, eviscerated, and fixed in 70% ethanol. An alizarin red/Alcian blue double-staining solution was used to distinguish calcified bone from cartilage for Prx1-cre$^{+/-}$;DTA$^{+/-}$ test (n = 4 mice) and Prx1-cre$^{-/-}$;DTA$^{+/-}$ controls (n = 6 mice).

Constitutive Lineage-Tracing Studies during Bone Regeneration

Prx1-cre$^{+/-}$ male mice were crossed with tdTOMATO$^{+/+}$ female mice to obtain Prx1-cre$^{+/-}$;tdTOMATO$^{+/-}$ male mice. A 100-μm defect was created by femtosecond laser ablation in the left frontal calvaria and right posterior calvaria of 8-week-old male mice. IVM was used to visualize PRX1-lineage cells at 0, 5, 10, and 30 days after creation of the defect (n = 3 mice).

Inducible Lineage-Tracing Studies during Heterotopic Suture Transplantation

Four-week-old Prx1-creER-EGFP$^{+/-}$;tdTOMATO$^{+/-}$ male mice (donors) were euthanized to provide tissue transplants to 4-week-old wild-type male mice (recipients). Coronal and sagittal sutures were excised from the donors, chopped into fine chips, mixed with Matrigel, and stored on ice. Using a drill with a 1-mm round bur, a 2-mm defect was created carefully (so as not to damage the underlying dura) in the left and right parietal bones of the recipient mice. The right defect was filled with suture chips + Matrigel or with Matrigel only. Animals were treated with 100 μL of tamoxifen in sterile oil (test, n = 3 mice) or sterile oil only (control, n = 2 mice) for 2 days (40 mg/kg, intraperitoneally) following surgery and then euthanized on day 28. Calvaria were prepared for histological fluorescent analysis.

Inducible Lineage-Ablation Studies during Subcritical Defect Regeneration

Eight-week-old, male Prx1-creER-EGFP$^{+/-}$;DTA$^{+/-}$ mice (test, n = 6 mice) and Prx1-creER-EGFP$^{-/-}$;DTA$^{+/-}$ mice (control, n = 6 mice) were injected with tamoxifen (intraperitoneally, 40 mg/kg in sterile oil) for 5 days before and 5 days after surgery. A 0.5-mm defect was made in the right parietal bone using a 0.5-mm round bur. Twenty-eight days after surgery, calvarial samples were fixed in 70% EtOH for micro-computed tomography (μCT) analysis and histological processing.

Inducible Lineage-Tracing Studies during Bone Regeneration

Eight-week-old, male Prx1-creER-EGFP$^{+/-}$;tdTOMATO$^{+/-}$ mice were injected with tamoxifen (intraperitoneally, 40 mg/kg in sterile oil) for 3 days before making a 100-μm defect using femtosecond laser ablation. IVM was performed at the time of the defect creation (t0), 5 days after (t5), 10 days after (t10) (n = 6 mice), and 60 days after (t60) (n = 2 mice).

Suturectomy Studies

Eight-week-old, male Prx1-creER-EGFP$^{+/-}$;tdTOMATO$^{+/}$ mice were used. Sutures were disrupted mechanically using a dental drill with a 0.25-mm diamond bur without perforating the dura. Bone defects (0.5 mm in diameter) were made 2 mm away from the sutures. Animals were euthanized 28 days after surgery and calvaria were dissected for histological processing (n = 5 mice/group).

Inducible Lineage-Tracing Studies during Orthotopic Suture Transplantation

Four-week-old, male Prx1-creER-EGFP$^{+/-}$;tdTOMATO$^{+/-}$ mice (donors) were euthanized to provide tissue to 4-week-old, male wild-type mice (recipients). The right coronal and sagittal sutures were excised from the donors and transplanted into an orthotopic site in recipient mice (after suturectomy). Six weeks after suture transplantation, a bone defect (0.5 mm in diameter) was made in the right parietal bone. Animals were injected with tamoxifen (intraperitoneally, 40 mg/kg in sterile oil) for 5 consecutive days to induce lineage tracing, and defects were imaged by IVM at days 7 and 14 postoperatively (n = 2 mice).

Single-Cell Clonogenicity Analysis

Four-week-old Prx1-creER-EGFP$^{+/-}$ mice were euthanized for EGFP^{+} cell isolation from coronal and sagittal sutures using fluorescence-activated cell sorting (FACS). 480 single EGFP^{+} or EGFP^{-} cells were sorted into five 96-well plates and cultured in basic medium (α-minimum essential medium [αMEM] supplemented with 20% fetal bovine serum [FBS] and 1% penicillin/streptomycin) for 3 weeks with medium changed twice per week. Cells were then washed with Earle's balanced salt solution, fixed in 3.7% paraformaldehyde, and stained with crystal violet for CFU-F analysis. Wells with more than 50 cells per colony were counted, (n = 3 independent experiments).

Ex Vivo qRT-PCR Analysis of PRX1-Expressing Cells

Four-week-old Prx1-creER-EGFP$^{+/-}$ or Col1-EGFP$^{+/-}$ mice were euthanized for EGFP^{+} cell isolation from coronal and sagittal sutures using FACS. Coronal and sagittal sutures were dissected, pooled, and digested at 37°C in a shaking water bath in two steps. First, with 3 mg/mL of collagenase II (Worthington Biochemical; cat. #LS004176) in αMEM and 1% penicillin/streptomycin for 90 min; then with 0.76 U/mL of collagenase P (Roche; cat. #11249002001), 0.67 U/mL of dispase (Worthington Biochemical; cat. #LS02104) in αMEM, and 1% penicillin/streptomycin for 30 min.

EGFP^{+} and EGFP^{-} cells were sorted (average of 10,000). Cell lysis, RNA isolation, and reverse transcription for gene expression analysis were performed using the Single Cell to CT kit (Thermo Fisher Scientific; cat. #4458237). qRT-PCR reactions were carried out using the TaqMan gene expression analysis technology. TaqMan assay codes for each gene primer set are listed in Table 1 (n = 3 independent experiments).

WNT Stimulation Studies

For in vitro studies, EGFP^{+} and EGFP^{-} cells were sorted by FACS from calvaria of newborn animals (n = 5–7 animals) and seeded into 6-well plates in basic medium (αMEM, 20% FBS, 1% penicillin/streptomycin) for cell culture. Cells (passage 4) were treated with either 50 ng/mL of rmWNt3a or 1,000 ng/mL of rmDDK1 (R&D Systems) and incubated for 48 hr, or pretreated for 24 hr with 1,000 ng/mL of rmDKK1 (R&D Systems) and then stimulated with 50 ng/mL of rmWNT3a (R&D Systems) for 48 hr. qRT-PCR was performed using TaqMan real-time PCR assays (Life Technologies) (n = 3 independent experiments). For in vivo studies, 7-day-old Prx1-creER-EGFP$^{+/-}$ animals received calvarial subperiosteal injections of rmWnt3a (440 ng/day in PBS, R&D Systems) (n = 6 mice) or control (PBS) (n = 5 mice) for 2 consecutive days. After 24 hr, EGFP^{+} cells were isolated from calvarial bones by FACS and qRT-PCR was performed using the Single Cell to CT kit (Thermo Fisher Scientific; cat. #4458237).

Inducible Lineage-Ablation Studies during Calvarial Development

Male Prx1-creER-EGFP$^{+/-}$;DTA$^{+/-}$ mice (3.5 weeks old; test, n = 4 mice) and Prx1-creER-EGFP$^{-/-}$;DTA$^{+/-}$ mice (control, n = 7 mice) were injected with tamoxifen (intraperitoneally, 40 mg/kg in sterile oil) for 5 days and then aged for 2 months. Mice were euthanized and the cranium was removed for μCT analysis and histological processing. Calvarial measurements were taken using AVISO 3D software (FEI North America) following methodologies described elsewhere (Richtsmeier et al., 2000). Long bone lengths were measured manually using a digital caliper. Methods were repeated for ablation of pnPRX1^{+} cells in 7-day-old animals (test n = 3, control n = 2).

Healing of Subcritical-Size Calvarial Defects after 2-Month Ablation of pnPRX1^{+} Cells

Male Prx1-creER-EGFP$^{+/-}$;DTA$^{+/-}$ mice (3.5 weeks old; test, n = 4) and Prx1-creER-EGFP$^{-/-}$;DTA$^{+/-}$ male mice (control, n = 2) were injected with tamoxifen (intraperitoneally, 40 mg/kg in sterile oil) for 5 days. Sixty days later, a 0.5-mm defect was made in the right parietal bone using a 0.5-mm round bur. Twenty-eight days after surgery, calvarial samples were fixed in 70% EtOH for μCT analysis and histological processing.

Comparative Localization of pnPRX1^{+} Cells and pnGLI1^{+} Cells

Male Prx1-creER-EGFP$^{+/-}$;tdTOMATO$^{+/-}$ and Gli1-creER$^{+/-}$;tdTOMATO$^{+/-}$ mice (3.5 weeks old) were injected with tamoxifen (intraperitoneally, 40 mg/kg in sterile oil) for 5 consecutive days

(short-pulsing, n = 2). On day 6, animals were euthanized and their mandibles were dissected for fluorescent histological analysis.

Statistics

Statistical analysis was performed using two-tailed distribution equal-variance Student's t test, and results are shown as means ± SD. Statistically significant difference is indicated in figures as *$p < 0.05$ or **$p < 0.01$.

SUPPLEMENTAL INFORMATION

Supplemental Information includes Supplemental Experimental Procedures and six figures and can be found with this article online at http://dx.doi.org/10.1016/j.stemcr.2017.03.002.

AUTHOR CONTRIBUTIONS

K.W., S.-C.A.Y., and L.J.M. equally contributed and performed the vast majority of the experiments described herein. Specifically: K.W. managed all mouse maintenance, cell isolations, in vitro cell culture and validation experiments, experimental design and execution of suturectomy, suture transplantation, and histology; S.-C.A.Yperformed IVM, suture transplantation, subperiosteal injections, and DTA ablation efficiency; and L.J.M. handled IVM, lineage tracing, bone defect studies, and suture cellularity studies. S.G. and S.H.B. performed the calvarial defect regeneration studies. C.M.L. performed histological evaluations and helped with technical aspects of multiple transgene expression analysis. Z.A.A. performed μCT analysis. C.P.L. and G.I. supervised the studies and directed the interpretations of the results.

ACKNOWLEDGMENTS

We acknowledge Dr. Shunichi Murakami (Case Western Reserve University) for kindly providing the Prx1-creER-EGFP mice, Dr. David Scadden (Harvard Stem Cell Institute) for providing the Col1-EGFP mice, Dr. Dolrudee Jumlongras and Dr. Bjorn Olsen (Harvard School of Dental Medicine) for providing the Gli1-creER; tdTOMATO mice, and Dr. Jenna Galloway (Massachusetts General Hospital) for sharing the collagenase-based cell isolation protocol. We thank Matthew Warman, Steven Hann, and Mark Kahan (Warman Lab at Children's Hospital of Boston) for their assistance with the preliminary Prx1-driven DTA ablation studies. We also thank Ronald Mathieu, Mahnaz Paktinat, and Yanhui Deng at the Children's Hospital & Harvard Stem Cell Institute Flow Cytometry Research Facility (Karp Research Labs, 1 Blackfan Circle, Boston) for their kind cooperation. We thank John R. Martin at the HSDM Micro CT Core Facility (188 Longwood Avenue, REB 316, Boston) and Daniel Brooks and Michael Armanini at the Harvard/MGH Center for Skeletal Research, Imaging and Biomechanical Testing Core for their technical assistance. This project was supported by grant no. R00DE021069 (NIH/NIDCR) to G.I. and by the HSDM Dean's Scholar Award to L.J.M. and S.-C.A.Y.

Received: August 30, 2016
Revised: February 28, 2017
Accepted: March 2, 2017
Published: March 30, 2017

REFERENCES

Baron, R., and Kneissel, M. (2013). WNT signaling in bone homeostasis and disease: from human mutations to treatments. Nat. Med. *19*, 179–192.

Chan, C.K., Seo, E.Y., Chen, J.Y., Lo, D., McArdle, A., Sinha, R., Tevlin, R., Seita, J., Vincent-Tompkins, J., Wearda, T., et al. (2015). Identification and specification of the mouse skeletal stem cell. Cell *160*, 285–298.

Chen, S., Lewallen, M., and Xie, T. (2013). Adhesion in the stem cell niche: biological roles and regulation. Development *140*, 255–265.

Cheung, T.H., and Rando, T.A. (2013). Molecular regulation of stem cell quiescence. Nat. Rev. Mol. Cell Biol. *14*, 329–340.

Cowan, C.M., Shi, Y.Y., Aalami, O.O., Chou, Y.F., Mari, C., Thomas, R., Quarto, N., Contag, C.H., Wu, B., and Longaker, M.T. (2004). Adipose-derived adult stromal cells heal critical-size mouse calvarial defects. Nat. Biotechnol. *22*, 560–567.

Du, B., Cawthorn, W.P., Su, A., Doucette, C.R., Yao, Y., Hemati, N., Kampert, S., McCoin, C., Broome, D.T., Rosen, C.J., et al. (2013). The transcription factor paired-related homeobox 1 (Prrx1) inhibits adipogenesis by activating transforming growth factor-β (TGFβ) signaling. J. Biol. Chem. *288*, 3036–3047.

Houlihan, D.D., Mabuchi, Y., Morikawa, S., Niibe, K., Araki, D., Suzuki, S., Okano, H., and Matsuzaki, Y. (2012). Isolation of mouse mesenchymal stem cells on the basis of expression of Sca-1 and PDGFR-α. Nat. Protoc. *7*, 2103–2111.

Jiang, X., Iseki, S., Maxson, R.E., Sucov, H.M., and Morriss-Kay, G.M. (2002). Tissue origins and interactions in the mammalian skull vault. Dev. Biol. *241*, 106–116.

Kalajzic, Z., Liu, P., Kalajzic, I., Du, Z., Braut, A., Mina, M., Canalis, E., and Rowe, D.W. (2002). Directing the expression of a green fluorescent protein transgene in differentiated osteoblasts: comparison between rat type I collagen and rat osteocalcin promoters. Bone *31*, 654–660.

Kawanami, A., Matsushita, T., Chan, Y.Y., and Murakami, S. (2009). Mice expressing GFP and CreER in osteochondro progenitor cells in the periosteum. Biochem. Biophys. Res. Commun. *386*, 477–482.

Kern, B., Shen, J., Starbuck, M., and Karsenty, G. (2001). Cbfa1 contributes to the osteoblast-specific expression of type I collagen genes. J. Biol. Chem. *276*, 7101–7107.

Lo Celso, C., Fleming, H.E., Wu, J.W., Zhao, C.X., Miake-Lye, S., Fujisaki, J., Cote, D., Rowe, D.W., Lin, C.P., and Scadden, D.T. (2009). Live-animal tracking of individual haematopoietic stem/progenitor cells in their niche. Nature *457*, 92–96.

Logan, M., Martin, J.F., Nagy, A., Lobe, C., Olson, E.N., and Tabin, C.J. (2002). Expression of Cre Recombinase in the developing mouse limb bud driven by a Prxl enhancer. Genesis *33*, 77–80.

Lu, X., Beck, J.G.R., Gilbert, L.C., Camalier, C.E., Bateman, N.W., Hood, B.L., Conrads, T.P., Kern, M.J., You, S., Chen, H., et al. (2011). Identification of the homeobox protein Prx1 (MHox, Prrx-1) as a regulator of osterix expression and mediator of tumor necrosis factor α action in osteoblast differentiation. J. Bone Miner. Res. *26*, 209–219.

Madisen, L., Zwingman, T.A., Sunkin, S.M., Oh, S.W., Zariwala, H.A., Gu, H., Ng, L.L., Palmiter, R.D., Hawrylycz, M.J., Jones,

A.R., et al. (2010). A robust and high-throughput Cre reporting and characterization system for the whole mouse brain. Nat. Neurosci. *13*, 133–140.

Mani, P., Jarrell, A., Myers, J., and Atit, R. (2010). Visualizing canonical Wnt signaling during mouse craniofacial development. Dev. Dyn. *239*, 354–363.

Martin, J.F., and Olson, E.N. (2000). Identification of a prx1 limb enhancer. Genesis *26*, 225–229.

Maruyama, T., Jeong, J., Sheu, T.J., and Hsu, W. (2016). Stem cells of the suture mesenchyme in craniofacial bone development, repair and regeneration. Nat. Commun. *7*, 10526.

Nakashima, K., Zhou, X., Kunkel, G., Zhang, Z., Deng, J.M., Behringer, R.R., and de Crombrugghe, B. (2002). The novel zinc finger-containing transcription factor osterix is required for osteoblast differentiation and bone formation. Cell *108*, 17–29.

Ouyang, Z., Chen, Z., Ishikawa, M., Yue, X., Kawanami, A., Leahy, P., Greenfield, E.M., and Murakami, S. (2014). Prx1 and 3.2kb Col1a1 promoters target distinct bone cell populations in transgenic mice. Bone *58*, 136–145.

Park, D., Spencer, J.A., Koh, B.I., Kobayashi, T., Fujisaki, J., Clemens, T.L., Lin, C.P., Kronenberg, H.M., and Scadden, D.T. (2012). Endogenous bone marrow MSCs are dynamic, fate-restricted participants in bone maintenance and regeneration. Cell Stem Cell *10*, 259–272.

Pinho, S., Lacombe, J., Hanoun, M., Mizoguchi, T., Bruns, I., Kunisaki, Y., and Frenette, P.S. (2013). PDGFRα and CD51 mark human nestin+ sphere-forming mesenchymal stem cells capable of hematopoietic progenitor cell expansion. J. Exp. Med. *210*, 1351–1367.

Richtsmeier, J.T., Baxter, L.L., and Reeves, R.H. (2000). Parallels of craniofacial maldevelopment in Down syndrome and Ts65Dn mice. Dev. Dyn. *217*, 137–145.

Sacchetti, B., Funari, A., Michienzi, S., Di Cesare, S., Piersanti, S., Saggio, I., Tagliafico, E., Ferrari, S., Robey, P.G., Riminucci, M., et al. (2007). Self-renewing osteoprogenitors in bone marrow sinusoids can organize a hematopoietic microenvironment. Cell *131*, 324–336.

Strecker, S., Fu, Y., Liu, Y., and Maye, P. (2013). Generation and characterization of Osterix-Cherry reporter mice. Genesis *51*, 246–258.

Tan, S.H., Senarath-Yapa, K., Chung, M.T., Longaker, M.T., Wu, J.Y., and Nusse, R. (2014). Wnts produced by Osterix-expressing osteolineage cells regulate their proliferation and differentiation. Proc. Natl. Acad. Sci. USA *111*, E5262–E5271.

Tsuji, K., Bandyopadhyay, A., Harfe, B.D., Cox, K., Kakar, S., Gerstenfeld, L., Einhorn, T., Tabin, C.J., and Rosen, V. (2006). BMP2 activity, although dispensable for bone formation, is required for the initiation of fracture healing. Nat. Genet. *38*, 1424–1429.

Voehringer, D., Liang, H.E., and Locksley, R.M. (2008). Homeostasis and effector function of lymphopenia-induced "memory-like" T cells in constitutively T cell-depleted mice. J. Immunol. *180*, 4742–4753.

Xiong, J., Onal, M., Jilka, R.L., Weinstein, R.S., Manolagas, S.C., and O'Brien, C.A. (2011). Matrix-embedded cells control osteoclast formation. Nat. Med. *17*, 1235–1241.

Yen, H.Y., Ting, M.C., and Maxson, R.E. (2010). Jagged1 functions downstream of Twist1 in the specification of the coronal suture and the formation of a boundary between osteogenic and non-osteogenic cells. Dev. Biol. *347*, 258–270.

Yu, H.M., Jerchow, B., Sheu, T.J., Liu, B., Costantini, F., Puzas, J.E., Birchmeier, W., and Hsu, W. (2005). The role of Axin2 in calvarial morphogenesis and craniosynostosis. Development *132*, 1995–2005.

Zegarelli, E.V. (1944). Adamantoblastomas in the slye stock of mice. Am. J. Pathol. *20*, 23–87.

Zhao, H., Feng, J., Ho, T.V., Grimes, W., Urata, M., and Chai, Y. (2015). The suture provides a niche for mesenchymal stem cells of craniofacial bones. Nat. Cell Biol. *17*, 386–396.